Journal of the Physical Society of Japan **86**, 114604 (2017)
https://doi.org/10.7566/JPSJ.86.114604

Acoustic Properties of Crystals with Jahn–Teller Impurities: Elastic Moduli and Relaxation Time. Application to SrF_2:Cr^{2+}

Nikita S. Averkiev[1], Isaac B. Bersuker[2], Vladimir V. Gudkov[3*†], Irina V. Zhevstovskikh[3,4], Maksim N. Sarychev[3], Sergei Zherlitsyn[5], Shadi Yasin[5‡], Gilman S. Shakurov[6], Vladimir A. Ulanov[7], and Vladimir T. Surikov[8]

[1]*A. F. Ioffe Physical Technical Institute of the Russian Academy of Sciences, 194021, St. Petersburg, Russia*
[2]*Institute for Theoretical Chemistry, The University of Texas at Austin, TX 78712, Austin, U.S.A.*
[3]*Ural Federal University, 620002, Ekaterinburg, Russia*
[4]*M. N. Miheev Institute of Metal Physics, Ural Branch of the Russian Academy of Sciences, 620137, Ekaterinburg, Russia*
[5]*Hochfeld-Magnetlabor Dresden (HLD-EMFL), Helmholtz-Zentrum Dresden-Rossendorf, D-01314 Dresden, Germany*
[6]*Kazan E. K. Zavoisky Physical-Technical Institute of the Russian Academy of Sciences, 420029, Kazan, Russia*
[7]*Kazan State Power Engineering University, 420066, Kazan, Russia*
[8]*Institute of Solid State Chemistry, Ural Branch of the Russian Academy of Sciences, 620990, Ekaterinburg, Russia*

(Received May 26, 2017; accepted September 19, 2017; published online October 16, 2017)

A new approach to evaluate the relaxation contribution to the total elastic moduli for crystals with Jahn–Teller (JT) impurities is worked out and applied to the analysis of the experimentally measured ultrasound velocity and attenuation in SrF_2:Cr^{2+}. Distinguished from previous work, the background adiabatic contribution to the moduli, important for revealing the impurity relaxation contribution, is taken into account. The temperature dependence of the relaxation time for transitions between the equivalent configurations of the JT centers has been obtained, and the activation energy for the latter in SrF_2:Cr^{2+}, as well as the linear vibronic coupling constant have been evaluated.

1. Introduction

Orbitally degenerate impurity centers in crystals, subjects to the Jahn–Teller (JT) effect, influence significantly a variety of observable properties of the latter, and ultrasonic experiments performed recently on II–VI:3*d* and III–V:3*d* crystals were shown to be very instrumental in the investigation of their structure and properties.[1–4)] Measurements of temperature dependent velocity and attenuation of the ultrasound waves allow one to reveal the main features of the adiabatic potential energy surface (APES) produced by the JT centers, including the linear and quadratic vibronic coupling constant, positions of the minima and saddle-points, the symmetry of the distorted configurations in the minima and the energy barrier between them. Since the energy of ultrasound phonons are too small to induce resonant transitions between the energy levels of the JT centers,[5)] only the ground state of the latter is involved in the interaction with the ultrasound wave, and its contribution to the complex elastic moduli is of relaxation origin. At low temperatures the mechanism of ultrasound relaxation may be described as follows: by reaching the JT center, the distortion amplitude of the ultrasound wave makes its (equivalent in equilibrium) JT distortions nonequivalent by exciting one or two of them, and then the system tends to return to equilibrium (relaxes) after the wave-maximum passes, transferring the excess energy to the phonons of the environment. At higher temperatures this relaxation becomes increasingly mediated by the crystal phonons.

Relaxation processes have been studied by ultrasound experiments in many systems (see, e.g., Refs. 6–11). It can be described in the framework of a phenomenological, approach,[12,13)] while a microscopic description of the Helmholtz free energy A or internal energy U establishes a bridge between the measured experimentally and revealed theoretically parameters of the system (see, e.g., Ref. 14). The elastic moduli are second derivatives of A or U with respect to the components of the deformation tensor. Assuming that the energy is an additive function of the crystal lattice and impurity centers, the total elastic moduli may be estimated as a sum of their contributions. To involve the formulas describing relaxation, we have to identify the contribution of the JT centers to the total tensor of elastic moduli $\mathbf{c}$; the components of the tensor c_{ij} are complex values which define the total attenuation α and the phase velocity v of the ultrasonic waves. Identification of the relaxation contribution of the JT centers c_{rel} is a challenging problem because the other contributions to the total elastic modulus, as a rule, are unknown, while the proper contribution of the JT centers c_{rel} is small, at least due to their small concentration ($n = 10^{17}$–10^{20} cm^{-3}).

Presenting time (t) and space ($\mathbf{r}$) dependence of the variables as $\exp[i(\omega t - \mathbf{k}\cdot\mathbf{r})]$, and introducing the wave number k as a complex variable, $k = \omega/v - i\alpha$ and assuming $|k| \gg \alpha$, we have:

$$\mathrm{Re}\, c = \rho v^2, \tag{1}$$

$$\mathrm{Im}\, c = 2\frac{c_0}{k_0}\alpha, \tag{2}$$

where ρ is the mass density. The subscript 0 in Eq. (2) relates to the real part of the variable defined at the reference temperature $T_0 \to 0$. Next, we assume that the total elastic modulus is a sum of the JT (relaxation) contribution and the background crystal lattice one: $c = c_{rel} + c_b$. Keeping only the first derivatives over time in the Zener equation,[12)] the relaxation process in the JT centers can be described as follows (see, e.g., Ref. 13):

$$\frac{1}{2}\frac{\mathrm{Re}\, c_{rel}}{c_0} = -\frac{\mathrm{Re}\, k_{rel}}{k_0} = \frac{v_{rel}}{v_0} = -\frac{1}{2}\frac{(c_{JT}^S - c_{JT}^T)}{c_0}\frac{1}{1+(\omega\tau)^2}, \tag{3}$$

$$\frac{1}{2}\frac{\mathrm{Im}\, c_{rel}}{c_0} = -\frac{\mathrm{Im}\, k_{rel}}{k_0} = \frac{\alpha_{rel}}{k_0} = \frac{1}{2}\frac{(c_{JT}^S - c_{JT}^T)}{c_0}\frac{\omega\tau}{1+(\omega\tau)^2}, \tag{4}$$

where the variables c, k, α, and v with subscript *rel* are defined similar to Eqs. (1) and (2), c_{JT}^{S} and c_{JT}^{T} are, respectively, the adiabatic and isothermal contributions of the JT centers to the total elastic modulus, ω is the cyclic frequency of the ultrasonic wave, τ is the relaxation time in the JT type relaxation described above.

An important feature in the manifestation of the JT effect in impurity crystals is the change of the relaxation time as a function of temperature $\tau(T)$ (at low temperatures) from that reflecting the activation mechanism (with over-the barrier transitions between APES minima) to the tunneling transitions through the potential energy barrier. It makes it possible to obtain the parameter of frequency dispersion $\omega\tau$, which becomes equal to a unity at a certain temperature T_1, $\omega\tau(T_1) = 1$, provided the experiment is carried out at sufficiently high frequencies, $\omega/2\pi > 10^6$ Hz. The condition $\omega\tau = 1$ is very specific. It separates the isothermal and adiabatic regimes, and as it follows from the Eqs. (3) and (4), a peak of attenuation and a step-like variation of the velocity occur at temperatures near $T = T_1$.

In dielectric and semiconducting crystals at low temperatures, the temperature dependence of the real and imaginary parts of c_b can be approximated by monotonic functions. Although the background attenuation $\alpha_b = (1/2)k_0 \operatorname{Im}(c_b/c_0)$ may be relatively large, its temperature variation is usually small in comparison with the peak of the impurity relaxation contribution $\alpha_{rel}(T)$. Moreover, α_b at $T < \theta_D/10$, where θ_D is the Debye temperature, is independent of temperature (see p. 52 in Ref. 15). It makes it possible to assume that α_b is a smooth function which coincides with the measured values of $\alpha(T)$ at $T \ll T_1$ and $T \gg T_1$. On the contrary, variation of $\operatorname{Re} c_b(T)$ (see, e.g., Ref. 16) may exceed variation of $\operatorname{Re} c_{rel}(T)$ (hence variation of v_b may exceed that of v_{rel}). Thus revealing $\operatorname{Re} c_b(T)$ (background stiffness) is much more difficult than the one for $\alpha_b(T)$. One of the approaches to this problem is to assume that $\operatorname{Re} c_b(T)$ is an even fourth-order polynomial of T.[17,18] In case of $\operatorname{Re} c_{rel}$ related to the impurity contribution, measurements on a relatively pure crystal (on a crystal without artificial doping) seem to ease the solution of this problem. Such a method of evaluating $\tau(1/T)$ based on data from velocity measurements, carried out on doped and un-doped crystals, was reported in Ref. 3. However, the procedure of doping may result in formation of other point defects, such as vacancies. Therefore the background acoustic properties of the doped crystals may differ from those in the temperature dependence of the attenuation and velocity (or elastic modulus) of the perfect un-doped crystal. The difficulties in determination of the relatively large and significantly temperature dependent background contribution to the velocity (or the real part of the modulus) is the main reason why most of the published ultrasonic experiments on crystals with JT impurities are focused on attenuation, and much less on the velocity of the ultrasound.

Meanwhile, the velocity measurements have some advantages over the attenuation experiments. Firstly, ultrasonic velocity is studied with the use of the phase-sensitive technique which has a high accuracy of about 10^6 (see, e.g., p. 11 in Ref. 15). Secondly, such experiments are less sensitive to micro cracks in bonds between the piezotransducers and specimens which occur during temperature changes affecting the attenuation measurements. Therefore, with the goal of increasing the accuracy of the results extracted from the experimental data (namely, the numerical values of the parameters of the APES of the JT centers), it seems to be very attractive to develop a method which relies on both ultrasound attenuation and velocity data.

In the present paper we develop such a new procedure of processing the data on $\alpha(T)$ and $v(T)$. This procedure allows for recovering the relaxation contributions to the attenuation and velocity. In addition, the isothermal and adiabatic elastic moduli, linear vibronic coupling constants, and activation energy are evaluated. The general approach is applied to the interpretation of the experimental results obtained on SrF_2:Cr^{2+} single crystals.

2. Relaxation Contribution to Elastic Modulus

As mentioned above, the peak of relaxation attenuation induced by the JT impurities exceeds the small variations of the background crystal lattice at low temperatures. The latter can be simulated with the help of a monotonic function which coincides with the total attenuation $\alpha(T)$ away from the relaxation peak.

To determine the temperature dependence of the background velocity v_b we apply the method introduced by Varshny[19] (see also p. 50 in Ref. 15 and references therein). Due to the an-harmonic phonon interactions the temperature dependence of the real part of the background elastic modulus is given by the following empirical expression:[19]

$$\frac{\Delta c_b}{c_0} = -\frac{s}{\exp(\theta/T) - 1}, \tag{5}$$

where s and θ are fitting parameters, $\Delta c_b = c_b(T) - c_0$, $c_0 = c(T_0)$, and T_0 is the reference temperature. Note that, written in the form of Eq. (5), c_b is defined as the *adiabatic modulus*. It means that it is a real and frequency independent value.

Following the approach applied for attenuation data, we should require that $\operatorname{Re} c(T) = c_b(T)$ for both $T \ll T_1$ and $T \gg T_1$. However, in fact the criterion $\operatorname{Re} c(T) = c_b(T)$ can be applied only under the condition of $T \ll T_1$ because the contribution to the elastic modulus from the JT centers, that vanishes at low temperatures, is nonzero at higher temperatures [see Eq. (3)]. Because of the latter we should assume that with the goal of ultrasound velocity investigations the background elastic modulus is different from the total one. Therefore, for the estimation of the fitting parameters s and θ in Eq. (5), in addition to the low temperature criterion analogous to that for attenuation,

$$\lim_{T\to 0} \frac{\operatorname{Re} c(T)}{c_b(T)} = 1, \tag{6}$$

we introduce new criteria that describe the main limitations in the relaxation contribution to the elastic modulus:

$$\operatorname{Re}[c_{rel}(T_1)] = -\operatorname{Im}[c_{rel}(T_1)], \tag{7}$$

$$\lim_{\frac{T_1}{T}\to 0} \frac{-\operatorname{Re} c_{rel}(T)T}{\operatorname{Im} c_{rel}(T_1)T_1} = 2 \tag{8}$$

Equations (7) and (8) follow directly from Eqs. (3) and (4) by taking in account that in our case the parameter $\omega\tau$ is temperature-dependent and increases with decreasing temperatures. Equation (8) is obtained assuming that $c_{JT}^{S} = 0$[14] and $c_{JT}^{T} \propto 1/T$ [see Eq. (23)].

3. Experiment

Experiments were carried out on SrF_2 crystals doped with Cr ions grown by Czochralski method in a helium atmosphere. A detailed EPR-study of these crystals[20] showed that the samples SrF_2:Cr contained mostly the bivalent chromium centers.

The Cr^{2+} dopants in cubic crystals with fluorite structure (e.g., SrF_2 BaF_2, CaF_2, CdF_2) replace the ions of the bivalent metal in the lattice site of the O_h-symmetry and are surrounded by the eight fluorine ions in the corners of the cube. The ground state of Cr^{2+} ion in the cubic coordination is orbitally threefold degenerate $^5T_{2g}$ subject to the $T_{2g} \otimes (e_g + t_{2g})$ JT problem with the APES defined in the five-dimensional space of the active tetragonal e_g and trigonal t_{2g} displacements.[21]

The concentration of Cr in the SrF_2 crystal was determined using an ELAN 9000 ICP-MS quadruple-based instrument (Perkin-Elmer SCIEX). It proved to be $n_{Cr} = (1.60 \pm 0.25) \times 10^{19}\,\mathrm{cm}^{-3}$.

Ultrasonic measurements were carried out at the Dresden High Magnetic Field Laboratory, Helmholtz-Zentrum Dresden-Rossendorf, Germany and at the Ural Federal University, Russia. The setups were operating as a frequency variable bridge (see p. 10 in Ref. 15 and p. 45 in Ref. 22). In these setups, the relative alternation of the frequency corresponding to the bridge balance is taken as $\Delta\omega/\omega_0 = \Delta v/v_0$, where $\Delta\omega = \omega(T) - \omega_0$, $\omega_0 = \omega(T_0)$, $\Delta v = v(T) - v_0$, $v_0 = v(T_0)$. Ultrasonic waves were generated and registered with the use of $LiNbO_3$ piezo-electric transducers at 56–105 MHz with the normal modes for all polarizations of the wave propagating along the [110] crystallographic axis. All the studied modes exhibit anomalies of relaxation origin but the biggest temperature variations of attenuation and velocity were obtained for the shear mode polarized along the [001] axis. This mode produces trigonal distortions of the JT complex and its attenuation and phase velocity are determined by the modulus c_{44}. Below we discuss only this mode, the discussion being carried out in terms of complex wave number and complex dynamic elastic modulus, omitting the subscript 44.

Figure 1 shows the experimental results obtained at the frequency $\omega/2\pi = 105$ MHz. The anomalies are of relaxation nature when the frequency dispersion parameter gets $\omega\tau = 1$ by varying the temperature.

The relaxation contribution to the complex wave number given by Eqs. (3) and (4) can be introduced in terms of the measured parameters as follows:

$$\mathrm{Re}\,\frac{k_{rel}}{k_0} = -\frac{v_{rel}}{v_0} = -2\,\frac{v_{rel}(T_1)\cdot T_1}{v_0 T}\,\frac{1}{1+(\omega\tau)^2}, \qquad (9)$$

$$\mathrm{Im}\,\frac{k_{rel}}{k_0} = -\frac{\alpha_{rel}}{k_0} = -2\,\frac{\alpha_{rel}(T_1)\cdot T_1}{k_0 T}\,\frac{\omega\tau}{1+(\omega\tau)^2}. \qquad (10)$$

Remind, k_{rel} and α_{rel} relate to the contribution of the impurity centers, whereas $v_0 = \sqrt{c/\rho}$ and $k_0 = \omega/v_0$ are defined by the total modulus c_0. In these expressions we took into account that $(c_{JT}^S - c_{JT}^T) \propto 1/T$.[14] This statement makes it possible to determine T_1: it corresponds to the maximum of the function $f(T) = -\mathrm{Im}\,k_{rel}(T)\cdot T$. The relaxation contribution to the imaginary part of the wave number (or imaginary part of the elastic modulus) can be obtained from the data on

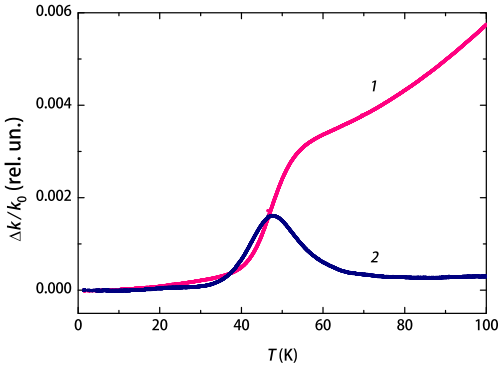

Fig. 1. (Color online) Temperature dependences of the wave number components; (1): $\mathrm{Re}\,\Delta k/k_0$, and (2): $-(\mathrm{Im}\,\Delta k/k_0) = [\alpha(T) - \alpha(T_0)]/k_0$. Denotations: $\Delta k = k(T) - k_0$, $k_0 = \omega/v(T_0)$, $T_0 = 1.4$ K.

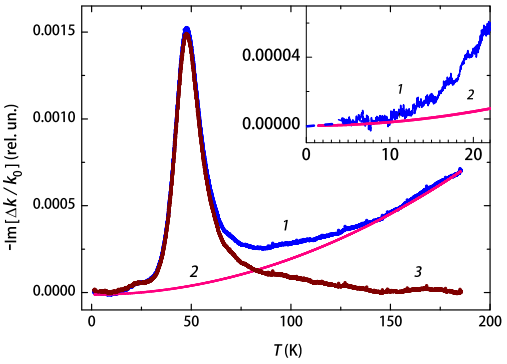

Fig. 2. (Color online) Temperature dependence of the imaginary part of the wave number $-\mathrm{Im}[\Delta k/k_0]$ (curve 1), background attenuation $\Delta\alpha_b/k_0$ (curve 2), and relaxation attenuation α_{rel}/k_0 (curve 3) at $\omega/2\pi = 105$ MHz. $-\mathrm{Im}\,\Delta k = \alpha(T) - \alpha_0$ with α_0 taken as extrapolation of $\alpha(T)$ to the zero temperature (the dased part of the curve 1 near $T = 0$ in the inset).

attenuation $\Delta\alpha = \alpha(T) - \alpha_0$ by extracting a monotonic function $[-\mathrm{Im}\,k_b(T)]$ which coincides with the measured curve at low and high temperatures (see Fig. 2). In our case we used $\mathrm{Im}\,k_b/k_0 = -\alpha_b/k_0 = -bT^2$ (where $b = 2.07 \times 10^{-8}\,\mathrm{K}^{-2}$) for the data measured at 105 MHz (given by the curve 2 in Fig. 2).

The criteria for simulation of the background contribution to the real part of the elastic modulus given by the Eqs. (6)–(8) actually represent the requirements for limited values in the functions $\mathrm{Re}[c_{rel}]T$ and $\mathrm{Im}[c_{rel}]T$. Presenting them in dimensionless forms we have:

$$\frac{1}{2}\,\frac{\mathrm{Re}\,c_{rel}}{\mathrm{Re}\,c_{rel}(T_1)}\,\frac{T}{T_1} = \frac{1}{4}\,\mathrm{Re}\,\frac{c_{rel}}{c_0}\,\frac{v_0}{v_{rel}(T_1)}\,\frac{T}{T_1} = \frac{1}{1+(\omega\tau)^2}, \qquad (11)$$

$$\frac{1}{2}\,\frac{\mathrm{Im}\,c_{rel}}{\mathrm{Im}\,c_{rel}(T_1)}\,\frac{T}{T_1} = \frac{1}{4}\,\mathrm{Im}\,\frac{c_{rel}}{c_0}\,\frac{k_0}{\alpha_{rel}(T_1)}\,\frac{T}{T_1} = \frac{\omega\tau}{1+(\omega\tau)^2}, \qquad (12)$$

where for small changes

$$\mathrm{Re}\,\frac{c_{rel}}{c_0} = 2\,\frac{\Delta v(T)}{v_0} - \frac{\Delta c_b}{c_0}, \qquad (13)$$

and

$$\frac{\mathrm{Im}\,c_{rel}}{c_0} = 2\,\frac{\Delta\alpha(T) - \alpha_b}{k_0}, \qquad (14)$$

with $\Delta v(T)/v_0$ and $\Delta\alpha(T)$ from the experimental data. We denote the right-hand-side functions in Eqs. (11) and (12) by φ_1 and φ_2, respectively.

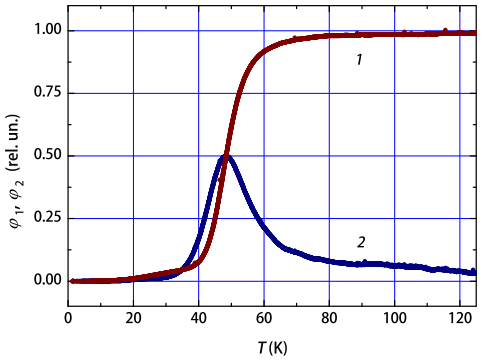

Fig. 3. (Color online) Fitting results: calculated temperature dependence of components of $c_{rel} \cdot T$, presented in the dimensionless form in the left-hand sides of Eqs. (11) and (12), coincide well with the functions $\varphi_1 = 1/[1 + (\omega\tau)^2]$ and $\varphi_2 = \omega\tau/[1 + (\omega\tau)^2]$, respectively.

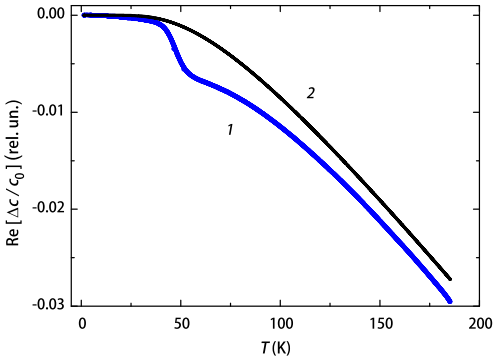

Fig. 4. (Color online) Temperature dependence of the real part of the dynamic elastic modulus c_{44} (curve 1) and fitting of its background contribution c_b (curve 2) defined by Eq. (5) with $s = 0.0495$ and $\theta = 192$ K.

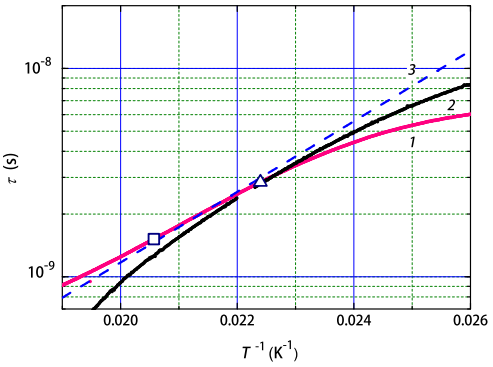

Fig. 5. (Color online) Temperature dependence of relaxation time obtained from the data on ultrasound velocity and attenuation at 105 MHz (curve 1) and 56 MHz (curve 2); the white square and triangle correspond to $\omega\tau = 1$ at 105 and 56 MHz, respectively, the dash line 3 follows equation $\tau = 0.48 \times 10^{-12} \exp(390/T)$.

Using Eq. (5) to determine the background contribution to the real part of the elastic modulus we obtained satisfactory results with the fitting parameters $s = 0.0495$ and $\theta = 192$ K: shown in Fig. 3, calculated with these parameters left-hand sides of Eqs. (11) and (12) follow well the right-hand-side functions φ_1 and φ_2. Note that the approximate choice of α_b is not very important: although it is included in α_{rel}, the latter is taken in Eq. (12) at $T = T_1$, where $\Delta\alpha(T_1) \gg \alpha_b(T_1)$. This statement is justified in Fig. 2 where the curves 1 and 3 represent total and relaxation attenuations, respectively. It is seen that these two curves have approximately equal maximum values.

The obtained value of $\Delta c_b(T)/c_0$ along with the total (dynamic) modulus measured at 105 MHz is given in Fig. 4. The adiabatic modulus c_b is frequency-independent, and hence, obtained from the experimental data at a certain frequency, it can be used to determine the relaxation contribution to the dynamic modulus at any other frequency.

4. Relaxation Time

After determining the relaxation contribution to the ultrasonic velocity $\Delta v_{rel}/v_0 = (1/2)\,\mathrm{Re}\, c_{rel}/c_0$ and attenuation α_{rel} we can evaluate the temperature dependence of the relaxation time based on the experimental data. Corresponding expressions can be derived from Eqs. (9) and (10):[13]

$$\tau = \frac{1}{\omega}\sqrt{2\frac{\Delta v_{rel}(T_1)\cdot T_1}{\Delta v_{rel}(T)\cdot T} - 1}, \tag{15}$$

$$\tau = \frac{1}{\omega}\left\{\frac{\Delta\alpha_{rel}(T_1)\cdot T_1}{\Delta\alpha_{rel}(T)\cdot T} \pm \sqrt{\left[\frac{\Delta\alpha_{rel}(T_1)\cdot T_1}{\Delta\alpha_{rel}(T)\cdot T}\right]^2 - 1}\right\}. \tag{16}$$

Naturally, the most reliable results can be obtained from the temperature interval corresponding to the most noticeable variation of the velocity and attenuation. Such variations occur in the vicinity of $T = T_1$ where the impurity contribution to the elastic modulus changes its form from isothermal to adiabatic, and the parameter of frequency dispersion $\omega\tau$ alternates from $\omega\tau < 1$ to $\omega\tau > 1$, respectively (or the function φ_1 changes from $\varphi_1 \approx 1$ to $\varphi_1 \approx 0$). We assume that the most reliable data (less sensitive to the choice of the background modulus c_b) correspond to the variation of φ_1 in the interval of 0.1–0.9 [with 10% difference from its low-temperature and high-temperature asymptotic values $\varphi_1(T \to 0) = 0$ and $\varphi_1(T \to \infty) = 1$, respectively]. According to the curve 1 given in Fig. 3 this temperature interval is approximately from 40 to 60 K (or $1/T$ values 0.025 and 0.017 K^{-1}).

The relaxation time as a function of the inverse temperature calculated with the use of Eq. (14) is shown in Fig. 5. In this temperature interval the dominant mechanism of relaxation is thermal activation, and the relaxation time is described as $\tau = \tau_0 \exp(V_0/T)$ (shown by dash line in Fig. 5). V_0 is the activation energy in K units. The value of the activation energy is defined by the slope of the curve $\tau(1/T)$ in semi-logarithmic scale in the vicinity of $1/T_1$ (square and triangle symbols in Fig. 5). Magnitudes derived from the data on ultrasonic velocity are: $V_0 = 390$ K (105 MHz) and $V_0 = 355$ K (56 MHz). They are in good agreement with the results obtained from the attenuation: $V_0 = 390$ K for both 56 and 105 MHz (for 56 MHz with the accuracy of about 10%).

The equation for the linear vibronic coupling constant can be revealed with the use of Eqs. (3), (4) keeping in mind $c_{JT}^S = 0$[14] and c_{JT}^T in the form of:

$$c_{JT}^T = \left(\frac{\partial^2 A_{JT}}{\partial\varepsilon^2}\right)_{\varepsilon=0} = -nk_BT\left(\frac{\partial^2 \ln Z}{\partial\varepsilon^2}\right)_{\varepsilon=0}, \tag{17}$$

where A_{JT} is the Helmholtz free energy of the JT centers, and k_B is the Boltzmann constant.

In the linear approximation, the operator of the potential energy of the vibronic Hamiltoniam contains two vibronic

coupling constants, F_E for tetragonal and F_T for trigonal symmetrized local displacements, or the analogous components of the deformation potential tensor b and d, respectively. The solution of the corresponding secular equation that contains also the initial elastic energy terms yields the adiabatic potential energy surface (APES) in the five-dimensional space of the symmetry coordinates. Three tetragonal and four trigonal extrema points of this surface are minima, whereas six orthorhombic extrema are saddle points. In the quadratic approximation with respect to the vibronic coupling terms the orthorhombic extrema points may become minima, while the tetragonal and trigonal ones transform into saddle points.[5,21] In our experiments, the JTE distortions are seen in both the trigonal c_{44} and tetragonal $c_{11} - c_{12}$ moduli. This means that the minima are of orthorhombic symmetry, in which the displacements along each of the three trigonal coordinates are accompanied by additional distortions along two tetragonal directions. The statement about orthorhombic distortions of the JT centers is in agreement with the results of EPR study of this crystal.[20] Accordingly, the vibronic energies of the complex related to such deformations are the following:

$$E_1 = E_2 = 0 \tag{18}$$

for the face perpendicular to the z-axis,

$$E_3 = b\frac{1}{2}\varepsilon_2 + d\sqrt{\frac{3}{2}}\varepsilon_4, \quad E_4 = b\frac{1}{2}\varepsilon_2 - d\sqrt{\frac{3}{2}}\varepsilon_4 \tag{19}$$

for the face perpendicular to the x-axis, and

$$E_5 = -b\frac{1}{2}\varepsilon_2 + d\sqrt{\frac{3}{2}}\varepsilon_4, \quad E_6 = -b\frac{1}{2}\varepsilon_2 - d\sqrt{\frac{3}{2}}\varepsilon_4 \tag{20}$$

for the face perpendicular to the y-axis.

For the trigonal modulus c_{44} the deformation ε in Eq. (17) is ε_4 and the partition function

$$Z = \sum_{i=1}^{6} \exp(-E_i/k_BT), \tag{21}$$

has the form of:

$$Z = 2 + \sum_{m,n=1}^{2} \exp\left\{\frac{-\left[(-1)^m d\sqrt{\frac{3}{2}}\varepsilon_4 + (-1)^n b\frac{1}{2}\varepsilon_2\right]}{k_BT}\right\}, \tag{22}$$

where b and d are the constants of the deformation potential. Hence, the discussed modulus is

$$c_{JT}^T = -\frac{nd^2}{k_BT}. \tag{23}$$

In our case $d = F_T a_0$, where F_T is the trigonal linear vibronic coupling constant, a_0 is the distance between the chromium and nearest fluorine ions. As a result we get:

$$F_T^2 = -\frac{4v_{rel}(T_1)k_BT_1c_0}{v_0 n a_0^2} = \frac{4\alpha_{rel}(T_1)k_BT_1c_0}{k_0 n a_0^2}. \tag{24}$$

Calculations carried out with $a_0 = 2.54$ Å, $c_0 = c_{44} = 3.308 \times 10^{11}$ dyn/cm^2, $v_0 = \sqrt{c_0/\rho}$, and $\rho = 4.3$ g/cm^3 yield $|F_T| = 3.71 \times 10^{-5}$ dyn.

Thus, obtained with two fitting parameters, $s = 0.0495$ and $\theta = 192$ K, satisfactory fitting of the functions $\varphi_1(T)$ and $\varphi_2(T)$ that describe the typical temperature dependence of the relaxation process, shows that the background attenuation (at least around $T = T_1$) is correctly defined. Such successful simulation of Δc_b with only two fitting parameters would be impossible if the background attenuation is determined incorrectly, and correction to the $\alpha_b(T)$ function, leading to changes in F_T and V_0 values, would be necessary. Hence exploration of both ultrasound attenuation and velocity data makes the result of evaluating the parameters of the APES of impurities in crystals more reliable.

5. Relaxed and Unrelaxed Elastic Moduli

The solution of the Zener equation,[12] derived keeping only the first derivatives over time can be expressed also in the following form (see, e.g., Ref. 13):

$$c_{rel} = c^T + (c^S - c^T)\frac{(\omega\tau)^2 - i\omega\tau}{1 + (\omega\tau)^2}, \tag{25}$$

$$c_{rel} = c^S - (c^S - c^T)\frac{1 - i\omega\tau}{1 + (\omega\tau)^2}. \tag{26}$$

In our case we assume that the background elastic modulus is adiabatic, and the JT impurity one is dynamic. Using Eqs. (25) and (26) in combination with Eqs. (3) and (4) we can express the isothermal and adiabatic moduli of the impurity subsystem as follows

$$\frac{c_{JT}^T}{c_0} = \frac{1}{c_0}\mathrm{Re}\left[c_{rel} - (c_{JT}^S - c_{JT}^T)\frac{(\omega\tau)^2 - i\omega\tau}{1 + (\omega\tau)^2}\right] = \mathrm{Re}\frac{c_{rel}}{c_0} + 2\frac{v_{rel}}{v_0}(\omega\tau)^2. \tag{27}$$

$$\frac{c_{JT}^S}{c_0} = \frac{1}{c_0}\mathrm{Re}\left[c_{rel} + (c_{JT}^S - c_{JT}^T)\frac{1 - i\omega\tau}{1 + (\omega\tau)^2}\right] = \mathrm{Re}\frac{c_{rel}}{c_0} - 2\frac{v_{rel}}{v_0} \equiv 0. \tag{28}$$

As above, we assume that c_0 is the dynamic modulus of the whole system in its low temperature limit [i.e., $c_0 = c(T \to 0)$]. To deduce the expressions for the relaxed and unrelaxed moduli, we should add $\Delta c_b/c_0$ to the right-hand and the left-hand parts of Eqs. (27) and (28). It makes it possible to obtain the frequency-independent moduli in the left-hand parts and to use the following relation in the right-hand parts:

$$\frac{\Delta c(T)}{c_0} = \frac{\mathrm{Re}\, c_{rel}}{c_0} + \frac{\Delta c_b}{c_0} = 2\frac{\Delta v(T)}{v_0}. \tag{29}$$

As a result we get:

$$\frac{\Delta c^R}{c_0} = \mathrm{Re}\left[\frac{c_{rel}}{c_0} + \frac{\Delta c_b}{c_0} - \frac{(c_{JT}^S - c_{JT}^T)}{c_0}\frac{(\omega\tau)^2 + i\omega\tau}{1 + (\omega\tau)^2}\right] = 2\left[\frac{\Delta v}{v_0} + \frac{\Delta v_{rel}}{v_0}(\omega\tau)^2\right]. \tag{30}$$

$$\frac{\Delta c^U}{c_0} = \mathrm{Re}\left[\frac{c_{rel}}{c_0} + \frac{\Delta c_b}{c_0} + \frac{(c_{JT}^S - c_{JT}^T)}{c_0}\frac{1 - i\omega\tau}{1 + (\omega\tau)^2}\right] = 2\left(\frac{\Delta v}{v_0} - \frac{\Delta v_{rel}}{v_0}\right). \tag{31}$$

The moduli in the left-hand parts of Eqs. (30) and (31)

$$\Delta c^R \equiv c^R - c_0 = c_{JT}^T + c_b \tag{32}$$

and

$$\Delta c^U \equiv c^U - c_0 = c_{JT}^S + c_b \tag{33}$$

can be considered as relaxed and unrelaxed ones.

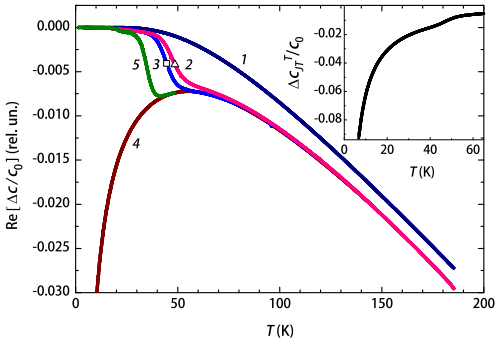

Fig. 6. (Color online) Temperature dependence of the dynamic modulus c_{44} (curves 2 for 105 MHz and 3 for 56 MHz), c_{44}^U (curve 1 for 105 MHz), and c_{44}^R (curve 4 for 105 MHz); the white square and triangle are defined in Fig. 5. The inset shows the isothermal contribution of the JT centers to the total elastic modulus c_{44}. Curve 5 is the dynamic modulus c_{44} calculated for $\Omega/2\pi = 5$ MHz with the use of Eq. (34) and experimental data on $\Delta v(T_1)$ and $\tau(T)$ at $\omega/2\pi = 105$ MHz; it shows the occurrence of a minimum in the $\mathrm{Re}\,\Delta c(T)/c_0$ value at lower frequencies.

The temperature dependences of the moduli calculated with the use of Eqs. (30) and (31), as well as the dynamic modulus, are shown in Fig. 6; the isothermal modulus associated with the impurity subsystem is given in the inset.

Usually the relaxed and unrelaxed moduli are related to the whole system, and they are synonyms of respectively isothermal and adiabatic moduli (see, e.g., Ref. 12). In our case this analogy is correct only regarding c^U since c_b is introduced as adiabatic one.

Despite of the fact that c^R does not describe the isothermal modulus of the system as a whole, the change from the relaxed to unrelaxed modulus at a certain temperature indicates the process of gradually freezing the JT centers in the APES minima. Moreover, c^R and c^U can be useful for interpretation of the experimental data, since they represent, respectively, the low and high frequency limits of the dynamic modulus $\mathrm{Re}\,c(\omega)$. As far as c^R and c^U are frequency independent, once determined at a given frequency they can be used for clear understanding the data obtained at any other frequencies. Particularly it is important if the monotonic dependence of $\mathrm{Re}\,\Delta c(T)/c_0$ is replaced by another one with a minimum at lower frequencies. Such a case can be illustrated by calculations for a certain frequency Ω using the following expression deduced from Eqs. (9) and (31) with $\Delta c^U/c_0$ obtained from the experimental data measured at $\omega > \Omega$:

$$\mathrm{Re}\,\frac{\Delta c(\Omega,T)}{c_0} = \frac{\Delta c^U}{c_0} + 4\,\frac{v_{rel}(\omega,T_1)\cdot T_1}{v_0\cdot T}\,\frac{1}{1+(\Omega\tau)^2} \qquad (34)$$

Note that in Eq. (34) the temperature T_1 is defined by the relation $\omega\tau = 1$, not $\Omega\tau = 1$.

6. Conclusion

A new approach to evaluate the relaxation contribution to the total elastic modulus of crystals with JT impurity centers, which takes into account the adiabatic background contributions to the total moduli, thus allowing for more accurate interpretation of ultrasound velocity measurements is reported. It has been applied for processing the experimental data on ultrasound velocity and attenuation obtained on SrF_2:Cr^{2+} single crystals in which relaxation occurs in the Cr^{2+} JT centers due to transitions between the equivalent distorted configurations in the minima of the APES. The temperature dependence of the relaxation time, relaxed and unrelaxed moduli, the magnitude of the activation energy for transition between the minima, and the linear trigonal vibronic coupling constant were evaluated based on the experimental results on ultrasound velocity and attenuation by applying this novel approach.

Acknowledgment The research was carried out with the state assignment of FASO of Russia (the theme "Electron" No. 01201463326), supported in part by RFBR (project 15-02-02750 a) and by UrFU Center of Excellence "Radiation and Nuclear Technologies" (Competitiveness Enhancement Program). The part of the work (N.S.Averkiev) was supported by the Goverment of Russia through the program P220 (project No. 14.Z50.31.0021, leading scientist M. Bayer). We also acknowledge the support from HLD at HZDR, member of the European Magnetic Field Laboratory (EMFL).

*gudkov@imp.uran.ru
†v.v.gudkov@urfu.ru
‡Present address: American University of the Middle East (AUM), College of Engineering and Technology, Eqaila, Kuwait

1) V. V. Gudkov, I. B. Bersuker, I. V. Zhevstovskikh, Yu. V. Korostelin, and A. I. Landmann, J. Phys.: Condens. Matter **23**, 115401 (2011).
2) N. S. Averkiev, K. A. Baryshnikov, I. B. Bersuker, V. V. Gudkov, I. V. Zhevstovskikh, V. Y. Mayakin, A. M. Monakhov, M. N. Sarychev, and V. E. Sedov, JETP Lett. **96**, 236 (2012).
3) V. V. Gudkov and I. B. Bersuker, in *Vibronic Interaction and the Jahn–Teller Effect. Theory and Applications*, ed. M. Atanasov, C. Daul, and Ph. L. W. Tregenna-Piggot (Springer, Dordrecht, 2012) p. 143.
4) N. S. Averkiev, I. B. Bersuker, V. V. Gudkov, K. A. Baryshnikov, I. V. Zhevstovskikh, V. Yu. Mayakin, A. M. Monakhov, M. N. Sarychev, V. E. Sedov, and V. T. Surikov, J. Appl. Phys. **116**, 103708 (2014).
5) I. B. Bersuker, *The Jahn–Teller Effect* (Cambridge University Press, Cambridge, U.K., 2006).
6) M. Weller, G. Y. Li, J. X. Zhang, T. S. Kê, and J. Diehl, Acta Metall. **29**, 1047 (1981).
7) A. Tamaki, T. Goto, S. Kunii, T. Suzuki, T. Fujimura, and T. Kasuya, J. Phys. C **18**, 5849 (1985).
8) Y. Nemoto, T. Goto, A. Ochiai, and T. Suzuki, Phys. Rev. B **61**, 12050 (2000).
9) T. Yanagisawa, P.-C. Ho, W. M. Yuhasz, M. B. Maple, Y. Yasumoto, H. Watanabe, Y. Nemoto, and T. Goto, J. Phys. Soc. Jpn. **77**, 074607 (2008).
10) I. Ishii, T. Fujita, I. Mori, H. Sugawara, M. Yoshizawa, K. Takegahara, and T. Suzuki, J. Phys. Soc. Jpn. **78**, 084601 (2009).
11) D. Yang, T. Chatterji, J. A. Schiemer, and M. A. Carpenter, Phys. Rev. B **93**, 144109 (2016).
12) C. Zener, *Elasticity and Anelesticity of Metals* (University of Chicago Press, Chicago, IL, 1948).
13) V. V. Gudkov, in *The Jahn–Teller Effect*, ed. H. Koppel, D. R. Yarkony, and H. Barentzen (Springer, New York, 2009) p. 743.
14) M. D. Sturge, in *Solid State Physics*, ed. F. Seitz, D. Turnbull, and H. Ehrenreich (Academic Press, New York, 1967) Vol. 20, p. 92.
15) B. Luthi, *Physical Acoustics in the Solid State* (Springer, Berlin, 2005).
16) V. V. Gudkov, A. T. Lonchakov, V. I. Sokolov, I. V. Zhevstovskikh, and V. T. Surikov, Sov. Phys. Solid State **50**, 176 (2008).
17) S. Kamikawa, I. Ishii, Y. Noguchi, H. Goto, T. K. Fujita, F. Nakagawa, H. Tanida, M. Sera, and T. Suzuki, J. Phys. Soc. Jpn. **85**, 074604 (2016).
18) X. Xi, I. Ishii, Y. Noguchi, H. Goto, S. Kamikawa, K. Araki, K. Katoh, and T. Suzuki, J. Phys. Soc. Jpn. **84**, 124602 (2015).
19) Y. P. Varshni, Phys. Rev. B **2**, 3952 (1970).
20) M. M. Zaripov, V. F. Tarasov, V. A. Ulanov, G. S. Shakurov, and M. L. Popov, Sov. Phys. Solid State **37**, 437 (1995).
21) I. B. Bersuker and V. Z. Polinger, Sov. Phys. JETP **66**, 2078 (1974).
22) V. V. Gudkov and J. D. Gavenda, *Magnetoacoustic Polarization Phenomena in Solids* (Springer, New York, 2000).